www.nature.com/scientificreports

scientific reports

OPEN

GIS-based monitoring of urban utility excavations for permit compliance and pavement management in smart cities

Mustafa Yurdabal Apak

Real-time compliance monitoring of urban utility excavations remains challenging in digital construction, pavement management, and infrastructure governance. This study presents a pilot field evaluation of a Geographic Information System–based Pavement and Infrastructure Monitoring System (GIS-PIMS) for permit verification, utility-proximity monitoring, and pavement management support. The framework integrates multi-sensor excavation-activity detection, GNSS-based equipment tracking, GIS-defined permit corridors, underground utility layers, and rule-based alarm logic. Field testing at three urban excavation sites used 30 paired observations comparing the tracking device with survey-grade RTK-GNSS reference measurements. The tracking unit showed a mean horizontal deviation of 6.82 m and an RMSE of 7.41 m. Under the tested 20 m-wide permit corridor, rule-based alarm classification achieved 96.7% accuracy. The findings support pilot-scale feasibility for spatial compliance screening, precautionary near-utility warning, and pavement reinstatement planning. Larger datasets, diverse equipment and urban conditions, and longer-term evaluation of communication reliability are required before citywide deployment.

Keywords GIS-based real-time monitoring, Remote inspection, Pavement management, Pavement reinstatement, Geofencing, Infrastructure resilience

Urban road networks are frequently subjected to excavation activities associated with the installation, maintenance, repair, and renewal of underground utility systems, including water, wastewater, natural gas, electricity, telecommunications, and drainage infrastructure. Although such interventions are essential for sustaining urban services, open-cut excavation remains one of the most disruptive practices especially in metropolitan areas. Repeated pavement cuts interrupt the structural continuity of asphalt pavement layers, disturb routine traffic flow, cause environmental impacts such as dust, noise, vibration, and may reduce the overall serviceability and safety of urban roads. Construction-related noise and vibration have also been shown to affect nearby residents and urban environmental quality[1].

Utility cuts are widely recognized as a significant contributor to premature pavement deterioration. Cutting and reinstating an existing pavement locally changes its structural composition and creates interfaces between the original pavement and the repaired trench area. When backfilling, compaction, drainage control, or asphalt reinstatement practices are inadequate, these sections may become vulnerable to differential settlement, surface unevenness, cracking along patch edges, water infiltration, rutting, and accelerated roughness development. Consequently, temporary or poorly restored trenches can reduce driving comfort, increase travel time, affect driver behavior, and create additional maintenance burdens for related road authorities. In this regard, excavation related pavement defects should be considered not only as localized construction consequences but also as factors influencing pavement asset value, traffic safety, road-user costs, and public satisfaction. A representative field example of such a temporary trench condition before permanent asphalt reinstatement is indicated in Fig. 1.

A further challenge arises from the institutional fragmentation of urban utility management. Multiple public and private stakeholders often operate within the same road corridors, while their asset inventories, permit workflows, construction schedules, and inspection practices may remain partially disconnected. Even when excavation permits are formally required, conventional compliance control generally relies on manual site inspections and post-event reporting. Such inspection driven workflows are labor-intensive, discontinuous, and

Department of Civil Engineering, Istanbul Gelisim University, Avcilar, Istanbul 34310, Turkey. email: myapak@gelisim.edu.tr; myapak@gmail.com

Fig. 1. Representative field view of a utility excavation trench left with temporary backfill before permanent asphalt reinstatement.

may fail to detect short time deviations, unauthorized excavations, or operations outside approved time and location limits. As a result, the same corridor may be excavated repeatedly by different utility agencies, newly restored pavements may be cut again, and existing underground infrastructure may be exposed to avoidable damage risks that may cause infrastructure service disruptions. More broadly, urban underground engineering studies emphasize that poorly coordinated underground works can affect urban functionality, environmental quality, and the efficient use of public space[2,3]. Since urban infrastructure systems are complex and need intensive capital, coordinated planning is also necessary to reduce duplicated works, service interruptions, and inefficient resource use[4].

Geographic Information Systems (GIS) and smart city technologies offer a suitable basis for addressing these limitations. GIS-based platforms can integrate permit geometries, underground utility layers, work orders, inspection records, and pavement management information within a common spatial environment. Previous studies have highlighted the role of GIS and spatiotemporal data models in utility work scheduling, permitting, municipal infrastructure management, and coordination among infrastructure stakeholders. Similarly, real-time equipment tracking, remote construction monitoring, and geofencing-based safety approaches have shown potential for detecting risky operations near underground assets. However, the effectiveness of such systems depends strongly on positioning accuracy, data reliability, and the integration of location information with verified permit and utility asset data. Furthermore, digital governance and smart city applications can reduce information asymmetry and improve institutional oversight in urban infrastructure operations[5].

Despite these advances, existing approaches generally address excavation related problems in a fragmented manner. Pavement management studies mainly focus on the deterioration and economic effects of utility cuts, whereas utility coordination studies emphasize scheduling and permitting. Geofencing-based studies mostly concentrate on proximity warnings or underground utility protection. Limited attention has been given to an integrated operational framework that simultaneously detects active excavation, verifies spatial and temporal permit compliance, monitors proximity to critical underground facilities, generates real-time alerts, and produces auditable geospatial records that can later support pavement reinstatement planning and municipal asset management.

This study proposes a Geographic Information System-based Excavation Tracking System integrated with a Pavement and Infrastructure Monitoring System (GIS-PIMS) to address this gap. The proposed framework combines sensor-based excavation activity detection, Global Navigation Satellite System (GNSS) based equipment positioning, GIS-based permit polygons or buffered corridors, underground utility asset layers, and rule-based alarm logic within a unified web-based platform. When excavation activity is detected, the system evaluates whether the construction machinery operates within the authorized spatial boundary, within the approved time window, and at a safe distance from critical underground utilities. Non-compliant or risky events are automatically recorded and communicated through warning mechanisms, thereby enabling timely intervention by the responsible municipal or utility authorities.

The novelty of this study lies in linking smart city-based excavation monitoring with permit-compliance governance and pavement-oriented reinstatement management. Unlike conventional permit systems that rely primarily on pre-approved documents and periodic field inspections, the proposed GIS-PIMS framework enables continuous, spatially explicit, and data-driven verification of excavation activities. In addition, the system creates a time-stamped geospatial audit trail that can support accountability, post-event investigation, cost recovery, and systematic pavement reinstatement planning. Therefore, the proposed approach provides an integrated framework intended to support the detection of unauthorized excavation activities, generate precautionary warnings near underground utilities, facilitate coordination among relevant authorities, and provide geospatial information for pavement reinstatement management.

It should be emphasized that, although utility cuts are associated with localized pavement deterioration, direct field assessment of physical pavement-condition indicators, including the Pavement Condition Index (PCI) and International Roughness Index (IRI), was beyond the scope of this pilot tracking study. Instead, the present work focuses on evaluating the geospatial monitoring and permit-compliance functions of GIS-PIMS and on establishing the time-stamped spatial audit trail required to support subsequent municipal pavement reinstatement management.

In addition to developing the proposed framework, this study evaluates its operational performance through field-based case studies conducted at different urban excavation sites. These case studies were designed to test whether the system could correctly identify excavation related events, assess compliance with authorized work zones, generate proximity-based warnings near critical utility lines, and produce auditable geospatial records under real operating conditions. The positioning performance of the tracking device was compared with RTK-GNSS reference measurements, and the implications of meter-level positioning deviations were assessed for geofencing reliability, false-alarm risk, and practical municipal deployment. Accordingly, this study contributes to the literature by demonstrating how excavation tracking can be transformed from a reactive inspection practice into a proactive, GIS-enabled, and pavement-oriented urban infrastructure management system. In this respect, the proposed GIS-PIMS framework also supports urban infrastructure resilience by reducing the likelihood of utility service disruptions, improving inter-agency coordination, and enabling timely pavement reinstatement after excavation activities.

Literature review

Urban utility excavations are widely recognized as one of the major causes of localized pavement deterioration in road networks, especially in metropolitan areas. Open-cut trenching interrupts the continuity of pavement layers and creates a repaired trench interface that may be vulnerable to settlement, cracking, roughness, water infiltration, and premature deformation when reinstatement quality is inadequate. Arudi et al. (2000) emphasized the need for systematic utility-cut management, while Eskandari Torbaghan et al. (2020) demonstrated the relationship between trenching practices and road deterioration[6,7]. Similarly, Transport Infrastructure Ireland (TII) (2020) reported that utility trenches along or across pavements may weaken the pavement structure and lead to settlement or cracking at reinstatement interfaces[8]. These defects can also influence traffic operation and user costs. Mallela and Sadasivam (2011) associated work-zone impacts with delay, vehicle operating costs, crash costs, emissions, and community effects, whereas Schroeder et al. (2015) discussed the mobility consequences of urban arterial work zones[9,10]. Wang et al. (2014) further showed that pavement roughness can affect free-flow speed and travel time[11]. In this context, Wilde et al. (2018) highlighted that frequent and uncontrolled utility cuts may cause congestion, roughness-related vehicle damage, and rapid pavement deterioration[12]. Recent studies have also strengthened this evidence. Ghosh et al. (2025) reported that pavement sections containing utility cuts deteriorated more than uncut sections and that the reduction in pavement condition index became more pronounced as the cut area increased[13]. Coni et al. (2024) similarly emphasized that utility cut patching can affect pavement structure through cracking, discontinuity, and interface-related deterioration[14]. At the urban scale, open-cut excavation also reflects a broader underground space management problem, because pavement structures and utility corridors interact within constrained rights-of-way[15]. Construction-related noise and vibration also affect nearby residents and environmental comfort, expanding the impact of utility works beyond pavement distress alone[1].

The management of utility excavations also requires effective coordination among road authorities, municipalities, and utility agencies. In practice, these stakeholders often operate with separate asset inventories, permit procedures, construction schedules, and inspection workflows, which may result in repeated excavations, delayed reinstatement, and avoidable damage to existing underground infrastructure[16,17]. GIS-based systems provide an effective basis for addressing these coordination problems. These systems can integrate utility networks, permit boundaries, road assets, work orders, and inspection data within a common spatial environment. Venigalla and Baik (2007) described GIS as a decision-support tool for municipal management, Balasubramani et al. (2020) emphasized its role in managing urban infrastructure datasets[18,19]. Tseng et al. (2011) proposed a spatiotemporal database approach for coordinating utility schedules, and Quiroga and Pina (2004) examined issues related to automated utility permitting[20,21]. Xu et al. (2020) further developed an automated right-of-way utility permitting model[22]. These studies demonstrate the importance of digital coordination. However, most existing systems mainly support planning, documentation, or approval processes rather than real-time verification of whether the actual excavation occurs within the approved location and time schedule. Urban underground space studies also indicate that underground corridors should be planned as part of land-use and infrastructure management, rather than as isolated utility interventions[2,3]. Since infrastructure systems are complex and capital-intensive, coordinated planning is essential for reducing duplicated works, service disruptions, and inefficient resource use[4].

Smart city and construction monitoring studies further indicate that sensor-based and real-time data systems can improve infrastructure governance. Angelidou (2016), Axelsson and Granath (2018), and Simonofski et al. (2021) emphasized the importance of integrated digital platforms and multi-stakeholder coordination in smart city development[23–25]. In construction monitoring, Rao et al. (2022) reviewed the use of sensors, positioning systems, and real-time data streams for site monitoring[26]. Einizinab et al. (2023) discussed remote and virtual inspection technologies[27]. All these studies suggest that excavation control can move beyond periodic field inspection toward continuous, data-driven monitoring. However, for excavation management, such monitoring should be linked not only to equipment tracking but also to GIS-based permit geometries, underground utility data, and pavement reinstatement workflows. In this context, digital governance and smart city applications can reduce information asymmetry and improve institutional oversight in urban infrastructure operations[5].

Geofencing and equipment tracking have particular relevance for preventing damage to underground utilities. Talmaki and Kamat (2014) proposed a real-time hybrid virtuality approach for preventing excavation-related utility strikes by integrating equipment location with underground utility information[28]. Asadollahi et al. (2018) similarly proposed a geofencing-based safety system for high-pressure pipelines, in which virtual protection zones are used to warn operators when excavation equipment approaches critical assets[29]. These studies show the potential of proximity-based warning systems. However, they also indicate that system reliability depends strongly on positioning accuracy. This issue is especially important in dense urban areas, where surrounding buildings and narrow street corridors may obstruct satellite signal reception and increase multipath-related positioning errors.

While individual technologies, such as GNSS fleet tracking, static GIS permit repositories, or proximity warning sensors, have been reported separately in the literature, existing approaches handle excavation management in a fragmented manner. Traditional tracking systems trigger frequent false alerts during non-excavation transit, whereas conventional GIS permit portals lack real-time field verification. To bridge this gap, the proposed GIS-PIMS framework introduces a closed-loop architecture that fuses multi-sensor machine telemetry with GIS permit corridors, underground utility layers, and municipal pavement reinstatement workflows within a single platform (Table 1).

Overall, the literature shows that utility-cut deterioration, GIS-based coordination, smart city monitoring, and geofencing-based safety have each been addressed from different perspectives. Nevertheless, these research streams have mostly developed separately. Limited attention has been given to an integrated framework that simultaneously detects active excavation, tracks construction machinery, verifies spatial and temporal permit compliance, monitors proximity to critical underground utilities, generates real-time alerts, and creates auditable geospatial records for pavement reinstatement and municipal asset management. The present study addresses this gap by proposing and field-testing a GIS-PIMS. By evaluating the system through case studies conducted at different urban excavation sites, this study positions excavation tracking as a proactive, GIS-enabled, and pavement-oriented urban infrastructure management approach rather than a reactive inspection practice.

Methodology

GIS-based excavation tracking system: architecture and working principle

The proposed GIS-PIMS was developed to support real-time monitoring, permit compliance verification, and risk-based warning generation during urban utility excavation activities. The system architecture integrates three main components: an excavation-activity detection unit mounted on the backhoe loader, a GNSS-based positioning and communication module, and a web-based GIS-PIMS platform in which permit geometries and underground utility assets are represented as spatial layers. Through this integration, excavation activities can be detected, georeferenced, transmitted to the central platform, and evaluated against predefined spatial and temporal constraints (Fig. 2).

The excavation activity detection component was designed to determine whether the construction machinery was actively engaged in excavation. For this purpose, motion and status sensors were installed on key components of the excavator, including the stabilizer legs, boom, bucket, and operator seat. The basic principle of the system is that excavation activity can be inferred when the machine enters a typical digging configuration, such as stabilizer deployment, operator presence, boom or bucket movement, and working-component motion consistent with excavation. The sensor signals are processed to generate a binary operational status, defined as active or inactive excavation. This approach enables the system to distinguish between ordinary vehicle movement and actual excavation activity.

To distinguish active excavation from general vehicle transit or non-excavation machinery operations, a multi-sensor logical classification logic was implemented on the onboard control unit. The activity detection framework integrates three physical sensor inputs:

- Stabilizer-Leg Status Sensor: An inductive switch detecting the mechanical lowering and ground-support engagement of the stabilizer legs.

System / feature	Standalone GNSS fleet tracking	Static municipal GIS permit portals	Geofencing-based safety systems	Proposed GIS-PIMS framework
Real-time machine telemetry	Included	No	Limited / application-dependent	Included
Physical activity detection (sensors: seat orientation, stabilizers, boom RMS)	No (Only vehicle motion)	No	No	Included (Multi-sensor fusion)
Automated permit boundary verification	No	Yes (Static/Offline)	Limited / application-dependent	Included (Real-time dynamic geofencing)
Underground utility proximity alerts	No	Partial (Visual map layer)	Included	Included (Rule-based automated risk alerts)
Pavement reinstatement support and audit logging	No	No	No	Included (Time-stamped geospatial trail)
Integrated operational decision support	No	No	No	Included (Operator display + Municipal dashboard)

Table 1. Comparative feature matrix between existing excavation monitoring approaches and the proposed GIS-PIMS framework.

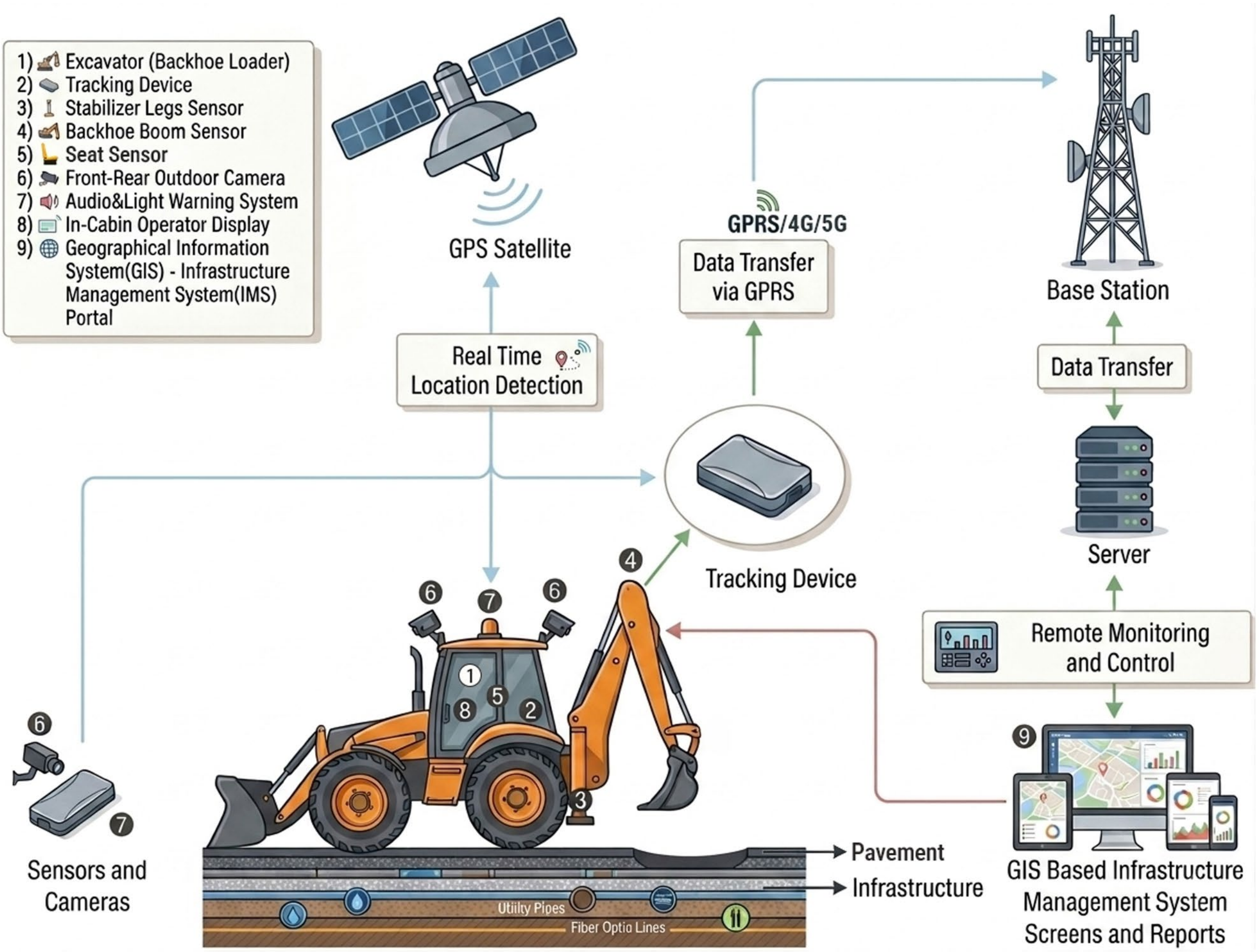

Fig. 2. Conceptual architecture of the GIS-PIMS-based excavation tracking and permit compliance monitoring framework.

- Boom/Bucket Motion Sensor: A tri-axial accelerometer mounted on the excavator arm, configured with a 10 Hz sampling frequency to capture dynamic angular rate variations and cyclic vibration signatures characteristic of digging.
- Operator-Seat Position and Occupancy Sensor: A seat-integrated switch mechanism that detects both operator occupancy and the 180° rotational orientation of the seat toward the backhoe/bucket operating position. On standard backhoe loaders, this ensures that activation is flagged only when the operator is physically seated and rotated facing the excavation controls.

Local sensor signals are sampled continuously at 10 Hz and processed over a 3-second sliding window. An "Active Excavation" operational state is binary-flagged (TRUE) when all three conditions are satisfied simultaneously: "*Seat Position == EXCAVATION_ORIENTED & OCCUPIED*, *Stabilizer Legs == DOWN*", and "*Boom Acceleration RMS > 0.3 g for >= 3 seconds*". If the operator seat is rotated toward the front driving position or any other condition remains unmet, the machine status is classified as non-excavation or transit (Fig. 3).

The onboard hardware installed in the excavator cabin functions as the central data acquisition, processing, authorization, and communication unit. The onboard control unit receives signals from the excavation activity sensors and combines these data with GNSS-based location information. The unit also includes communication interfaces, a SIM card module for cellular data transfer, camera interfaces for visual verification, auxiliary input/output ports, and a GNSS/GPS antenna connection. A dedicated operator display provides real-time feedback regarding the current system status and alarm condition. In addition, an RFID-based authorization unit is used to verify the operator or operation before excavation begins. Under the proposed workflow, excavation can proceed only when the operator or operation is recognized within the designated work zone and verified by the responsible authority (Fig. 4).

The location of the excavator is continuously monitored using GNSS positioning. The time-stamped activity and location data are transmitted to the GIS-PIMS server through cellular communication and visualized on the web-based GIS interface. In the GIS-PIMS environment, the authorized excavation area is digitized either as a permit polygon or as a buffered corridor along the planned utility alignment. In addition to permit geometries, underground utility assets such as natural gas, water, electricity, fiberoptic, and other critical infrastructure lines

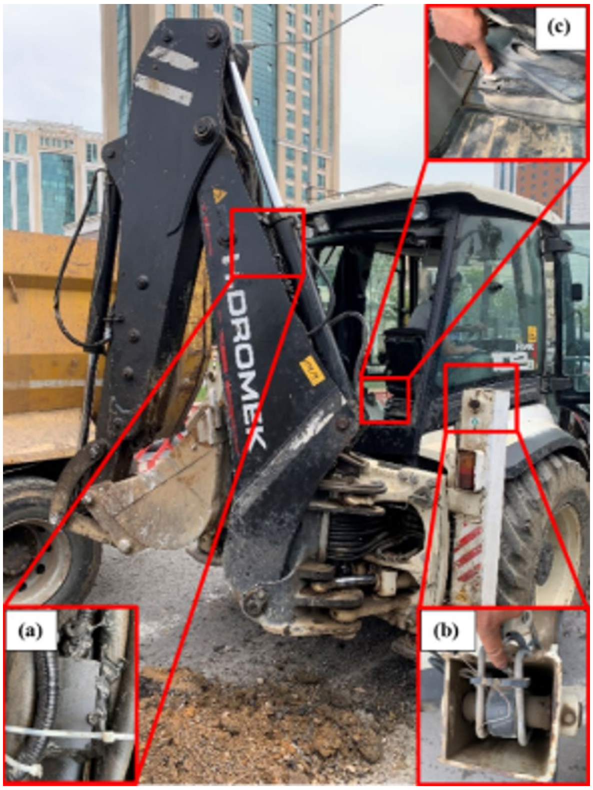

Fig. 3. Sensor configuration for detecting active excavation status on the construction machinery (**a**) boom-mounted motion sensor, (**b**) stabilizer-leg status sensor, and (**c**) operator-seat occupancy sensor.

are integrated into the platform as GIS layers. This spatial database enables the system to evaluate whether an active excavation occurs within the approved work zone and whether it is located near critical underground facilities.

The operational workflow begins with the submission and approval of an excavation permit through the GIS-PIMS platform. After approval, the permitted excavation boundary, planned route, validity period, and relevant permit attributes are stored in the system. During field operation, the GIS-PIMS engine first checks whether the excavator is in an active excavation state. If active excavation is detected, the system evaluates the incoming location data according to a rule-based decision sequence. This sequence includes verification of the existence of a valid permit, assessment of whether the excavator is located within the permitted area or buffer zone, confirmation of whether the activity occurs within the authorized time window, and evaluation of the excavator's proximity to critical underground utility lines (Fig. 5).

The rule-based compliance engine was activated only when the multi-sensor configuration indicated an active excavation state. Spatial compliance was assessed by evaluating the incoming GNSS coordinates against the GIS-defined permit corridor. In the pilot implementation, the authorized excavation zone was defined by applying a 10 m lateral offset to both sides of the planned utility centerline, creating a 20 m total permit corridor width. A tracked position located inside or on the boundary of this corridor was classified as spatially compliant, whereas a position outside the corridor generated an out-of-permit warning. No additional spatial tolerance was applied beyond this predefined 20 m corridor. Temporal compliance was verified by comparing the timestamp of each active excavation event with the approved permit start and end times; activities falling outside the authorized time window were recorded under the general permit non-compliance condition. Utility proximity was calculated as the shortest horizontal distance (d) between the tracked excavation position and the relevant underground utility layer, and a near-utility warning was generated when this distance (d) was equal to or less than 6 m. Events that were simultaneously outside the authorized corridor and within the utility-proximity threshold were recorded as combined higher-risk conditions. Communication-status failures were recorded separately because loss of cellular connectivity affects alarm transmission rather than the underlying spatial classification. The operational parameters, decision logic, and output classifications governing this rule-based evaluation are summarized in Table 2.

The alarm logic of the system is based on the combination of excavation activity status, spatial compliance, temporal validity, institutional authorization, and proximity to critical utilities. If excavation activity is detected without an approved permit or without institutional authorization, the system generates a no-authorization or unlicensed excavation alert. If the excavator is operating outside the approved permit polygon or buffer corridor, an out-of-permit excavation alert is generated. If the excavator is operating near a critical underground utility

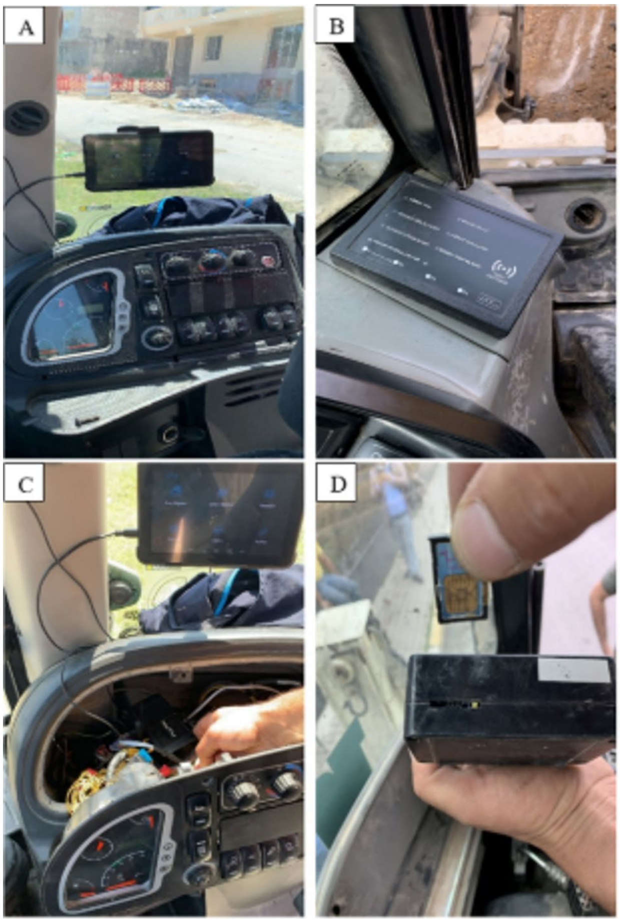

Fig. 4. Onboard hardware configuration of the excavation tracking unit (**a**) in-cab operator display, (**b**) RFID-based authorization reader, (**c**) onboard control unit, (**d**) cellular communication module.

line, a near-utility excavation alert is generated. When the excavator is both outside the permitted work zone and near a critical utility line, the event is escalated as a higher-risk out-of-permit near-utility alert.

The generated alerts are communicated through multiple channels, including the in-cab operator display, SMS, and e-mail notifications to responsible stakeholders. This multi-channel warning mechanism is intended to provide immediate feedback to the operator and enable timely intervention by municipal or utility authorities. Depending on the operational protocol and alarm confirmation process, excavation may either continue under controlled conditions or be halted until the alarm status is verified. In this respect, the system does not only function as a tracking tool but also as a decision-support mechanism for excavation governance.

A key output of the GIS-PIMS framework is the creation of a time-stamped geospatial audit trail. Each excavation-related event is recorded with its location, time, activity status, permit condition, alarm type, and responsible operator or institutional information. These records can later be used for compliance assessment, post-event investigation, cost recovery, pavement reinstatement planning, and coordination among utility agencies. In addition, the same event records can support pavement management by identifying where and when excavation activities occurred, thereby enabling authorities to link excavation records with subsequent pavement defects, reinstatement delays, complaints, or maintenance needs.

Overall, the working principle of the proposed system is based on transforming excavation management from a reactive inspection process into a proactive, GIS-enabled, and data-driven monitoring framework. By integrating excavation activity detection, GNSS-based equipment tracking, permit geometry control, underground utility proximity assessment, and automated warning generation, the system provides a practical tool for reducing unauthorized excavation, preventing damage to critical infrastructure, improving inter-agency coordination, and supporting timely pavement reinstatement.

Field case studies and system validation

Field-based case studies were conducted to validate the operational performance of the proposed GIS-PIMS framework under real urban excavation conditions. The validation procedure was designed to examine how the system records excavation-related spatial events, represents permitted excavation zones within the GIS environment, and compares the tracking outputs of the excavation vehicle with high accuracy reference measurements. In this section, the field validation setup, reference measurement procedure, test locations, and geospatial data preparation are described.

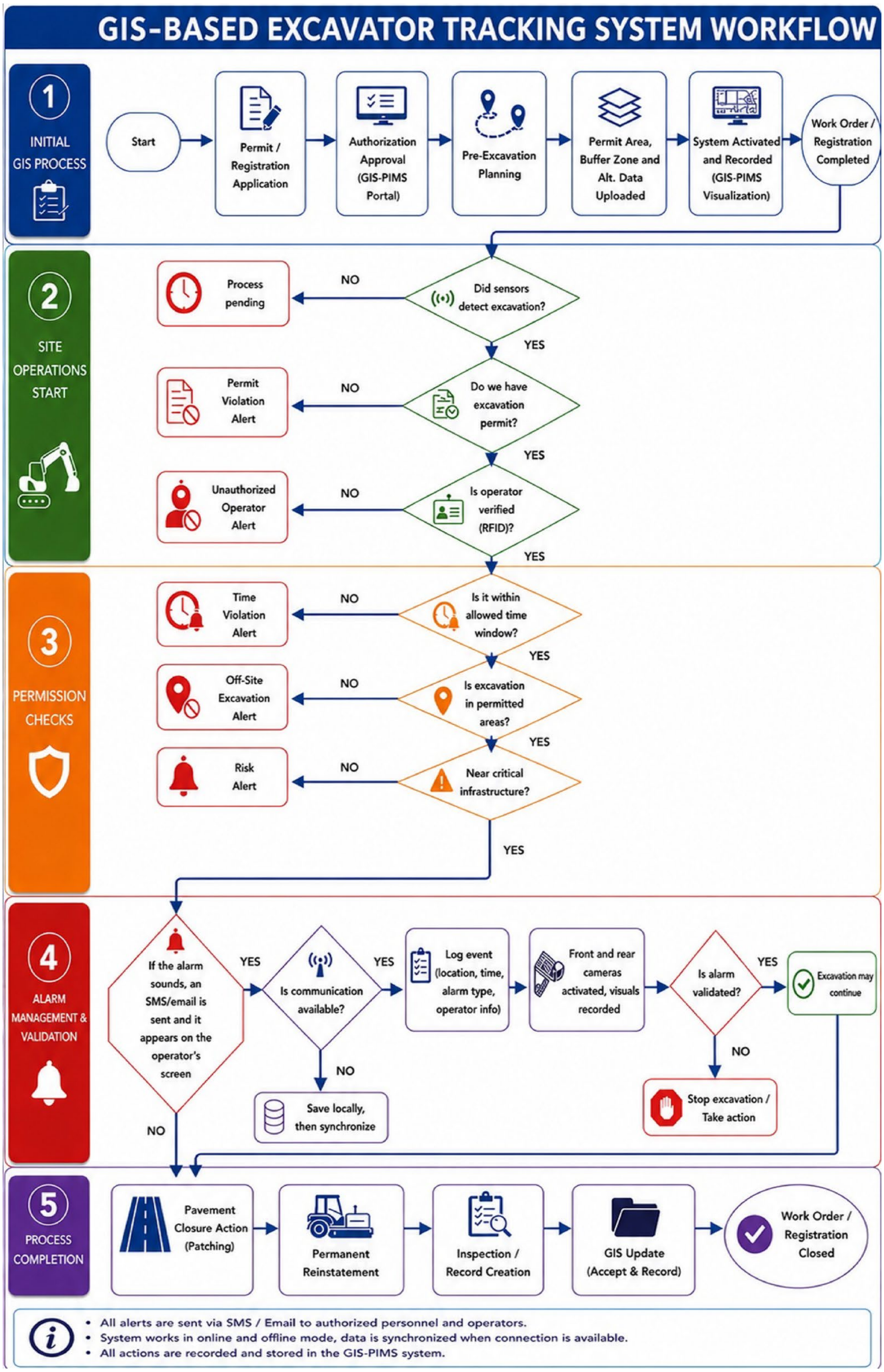

Fig. 5. Rule-based GIS-PIMS workflow for excavation activity detection, spatial temporal permit compliance verification, proximity assessment, and alert generation.

Parameter	Operational definition	Decision rule	System output
Excavation activity status	Active excavation state derived from operator seat, stabilizer legs, and boom/arm sensors	Compliance rules are evaluated only when the excavation status is active	Active/inactive excavation status
Permit validity	Existence of an active approved permit linked to the operation	No valid permit record → non-compliant operation	Unlicensed excavation warning
Institutional/operator authorization	Verification of operator or utility entity via RFID / digital authorization	No valid authorization → non-compliant operation	Unauthorized operator warning
Permit-corridor buffer	10 m lateral offset applied to both sides of the utility centerline (20 m total width)	Defines the authorized spatial work zone accommodating GNSS uncertainty	Inside / Outside corridor classification
Geofence spatial tolerance	No additional spatial tolerance applied beyond the defined 20 m corridor	Direct point-in-polygon evaluation against the corridor boundary	Direct spatial violation trigger
Authorized time window	Approved permit operational schedule (dates and daily hours)	Active excavation timestamp within the approved interval → temporally compliant; timestamp outside the interval → temporal non-compliance	Time-window/permit-compliance warning
Utility-proximity threshold	Shortest horizontal distance (d) between the tracked excavation position and a critical underground utility	$d \leq 6$ m during active excavation	Near-utility excavation warning
Combined spatial and proximity violation	Excavation occurs outside the permit corridor and within 6 m of a critical utility	Both conditions satisfied simultaneously	Escalated high-risk out-of-permit near-utility warning
Communication status	Availability of cellular data transmission	Loss of cellular communication is recorded separately from the spatial alarm decision	Communication-failure status log

Table 2. Rule-based compliance parameters and decision logic.

In the field validation process, the coordinates reported by the tracking device mounted on the excavation vehicle and visualized in the GIS-PIMS portal were compared with reference coordinates obtained using a survey-grade GNSS receiver. The GeoMax Zenith 25 Pro receiver was operated in RTK-fixed mode using real-time correction data. Only coordinates obtained after achieving a fixed ambiguity solution were accepted as reference measurements. During the field application, the reference coordinates obtained from the GNSS receiver and the coordinates reported by the excavation vehicle tracking device were collected simultaneously at the selected measurement points (Fig. 6).

The RTK-fixed coordinates obtained from the GeoMax Zenith 25 Pro receiver were used as the reference dataset because their expected horizontal uncertainty was substantially smaller than the meter-level error of the tracking device. The RTK-GNSS receiver provides millimeter-level horizontal accuracy, specified as 5 mm + 0.5 ppm RMS, whereas the tracking device used in the pilot deployment operates at meter level accuracy, with a reported error range of approximately 2.5–6 m. Therefore, the error associated with the reference RTK-GNSS measurements was considered negligible compared with the expected deviations of the tracking device. Accordingly, the horizontal position error of the tracking device was calculated as the planimetric distance between each tracked coordinate and its corresponding GNSS reference point.

To capture varying GNSS multipath and satellite occlusion conditions, the field validation was conducted across three distinct urban street morphologies in Istanbul. Cebesoy Street and Niyaz Street represent narrow, dense urban corridors with street widths of approximately 8–10 m and surrounding high-rise residential structures of 6 to 12 stories, inducing severe satellite signal obstruction and multipath reflections. In contrast, Kayışdağı Avenue represents a wide arterial corridor with a total width of approximately 25–30 m and low-rise building obstruction, serving as an open-sky baseline. All field campaigns were conducted under clear and dry weather conditions without precipitation.

These locations were selected because they represented active urban utility work zones where excavation monitoring, permit boundary verification, and proximity assessment to existing underground infrastructure were operationally relevant. A total of 30 positioning measurements were collected over three field days, with 10 paired measurements obtained at each site. For each measurement, the tracking device coordinate and the GNSS reference coordinate were recorded simultaneously to allow direct comparison between the two positioning outputs (Fig. 7).

Across the three selected sites, field data acquisition was carried out over three operational field days, with continuous monitoring lasting approximately 3 to 4 h per day during active municipal natural gas utility trenching operations. The field evaluation captured distinct physical excavation cycles including bucket digging, backhoe swing, and temporary trenching. During active excavation cycles, paired measurements were recorded at 15-minute intervals while the excavator was temporarily stationary, thereby minimizing kinematic mismatch between the tracking-device output and the RTK-GNSS reference measurement. Timestamp synchronization between the third-party vehicle tracking unit and the reference RTK-GNSS receiver was maintained via UTC time-stamping logged at the central server. All coordinates and GIS layers were transformed into the WGS 84 / UTM zone 35 N coordinate reference system (EPSG:32635) before planimetric distance and spatial-classification calculations were performed.

The commercial vehicle tracking device antenna was rigidly mounted on the top exterior of the excavator cabin structure to maximize sky visibility. For ground-truth validation, the survey-grade GeoMax Zenith 25 Pro RTK-GNSS antenna was positioned on a survey range pole aligned with the vertical axis of the tracking unit antenna. The RTK-GNSS receiver received real-time kinematic differential corrections from the ISKI-CORS (NRTK) network via cellular connection. Measurement points were selected based on operational safety, active excavation state, and spatial proximity to underground infrastructure lines. Positioning coordinates were

Fig. 6. Field validation procedure used to compare GIS-PIMS tracking outputs with survey-grade RTK-fixed GNSS reference measurements.

logged only after achieving a verified RTK-Fixed ambiguity solution with an internal horizontal accuracy status threshold of < 15 mm.

The authorized excavation area was represented in the GIS-PIMS platform as a buffered permit corridor along the planned utility alignment. In the pilot implementation, the authorized excavation area was delineated by applying a 10 m lateral buffer to each side of the planned utility centerline, thereby creating a permit corridor with a total width of 20 m. This buffered permit geometry served as the spatial reference for geofencing

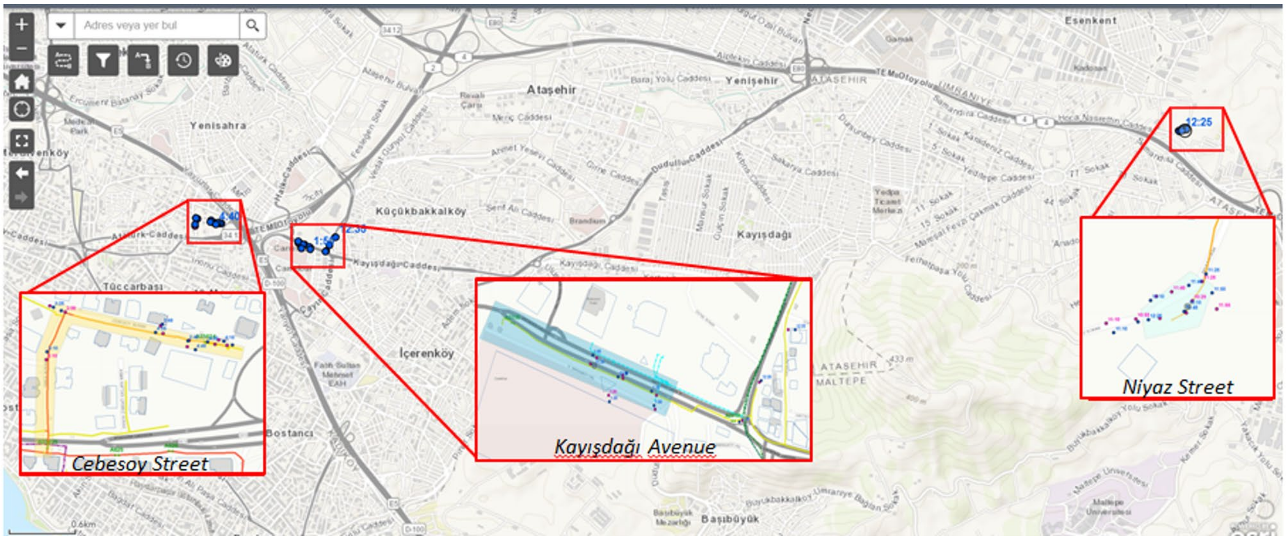

Fig. 7. Spatial distribution of the urban field case study locations selected for GIS-PIMS positioning and operational validation. The map was created by the author using Esri ArcGIS Web AppBuilder 2.21 in ArcGIS Online (June 2021 release; Esri, Redlands, CA, USA). Basemap credits: Esri, HERE, Garmin, INCREMENT P, and USGS. Software URL: https://doc.arcgis.com/en/web-appbuilder/.

verification and enabled the system to determine whether the tracked excavation activity occurred within the authorized work zone.

In addition to the permit corridor, existing and newly installed underground utility lines were integrated into the GIS-PIMS environment as spatial layers. In the GIS-PIMS visualization, the paired tracking and reference points were displayed together with the buffered excavation permit area and underground utility layers. The reference coordinates obtained from the GNSS receiver and the coordinates reported by the tracking device were shown as separate point layers, allowing visual comparison of the positional outputs. The platform also displayed relevant event attributes, including timestamp information and alarm/status fields, through the GIS-PIMS interface (Fig. 8).

The validation dataset included time-stamped tracking device coordinates, corresponding survey grade GNSS reference coordinates, horizontal deviations, permit corridor geometry, and proximity related spatial information associated with underground utility lines. The positioning performance of the tracking device was assessed using descriptive error statistics, including mean, standard deviation, range, root mean square error, and percentile-based indicators of horizontal deviation, thereby characterizing both the central tendency and dispersion of positioning errors observed during field validation.

The horizontal deviation data from the combined dataset of 30 paired observations were evaluated for normality using a one-sample Kolmogorov–Smirnov test to support distribution-based interpretation, supplemented by graphical diagnostics including a normal probability plot and a box plot. Statistical significance was set at $p < 0.05$. The deviation distribution was also assessed relative to the tracking device's specified 6 m deviation limit by calculating the observed exceedance rate, defined as the percentage of measurements with deviations greater than 6 m. For comparative interpretation, the expected exceedance rate under the fitted normal model was estimated using the sample mean and standard deviation, providing the statistical basis for evaluating positioning reliability, geofencing uncertainty, and proximity warning performance.

Results and discussion

Site-specific positioning accuracy and alarm outcomes

The field validation results were evaluated separately for the three urban excavation case study locations (Niyaz Street, Cebesoy Street, and Kayışdağı Avenue). At each site, ten paired observations were obtained by simultaneously recording the coordinates reported by the excavation vehicle tracking device and the corresponding reference coordinates measured using the GNSS receiver. The horizontal deviation was calculated as the planimetric distance between the two coordinate sets. In addition to positioning deviation, the distance of the tracked and reference points to the critical utility line and the alarm outcome generated by the GIS-PIMS framework were also recorded.

Niyaz street case study

The results obtained from the Niyaz Street field test are presented in Table 3, and the spatial distribution of the paired measurement points is shown in Fig. 9. The observed horizontal deviations ranged from 1.66 m to 11.68 m, with a mean deviation of 6.26 m, a median of 6.27 m, a root mean square error of 7.04 m, and a 95th percentile value of 11.14 m. These results indicate that the tracking device provided meter-level positioning accuracy under the tested urban conditions. To quantitatively evaluate system performance, each observation was classified under "Alarm Conditions" into standard confusion matrix categories (e.g., True Positive (TP)

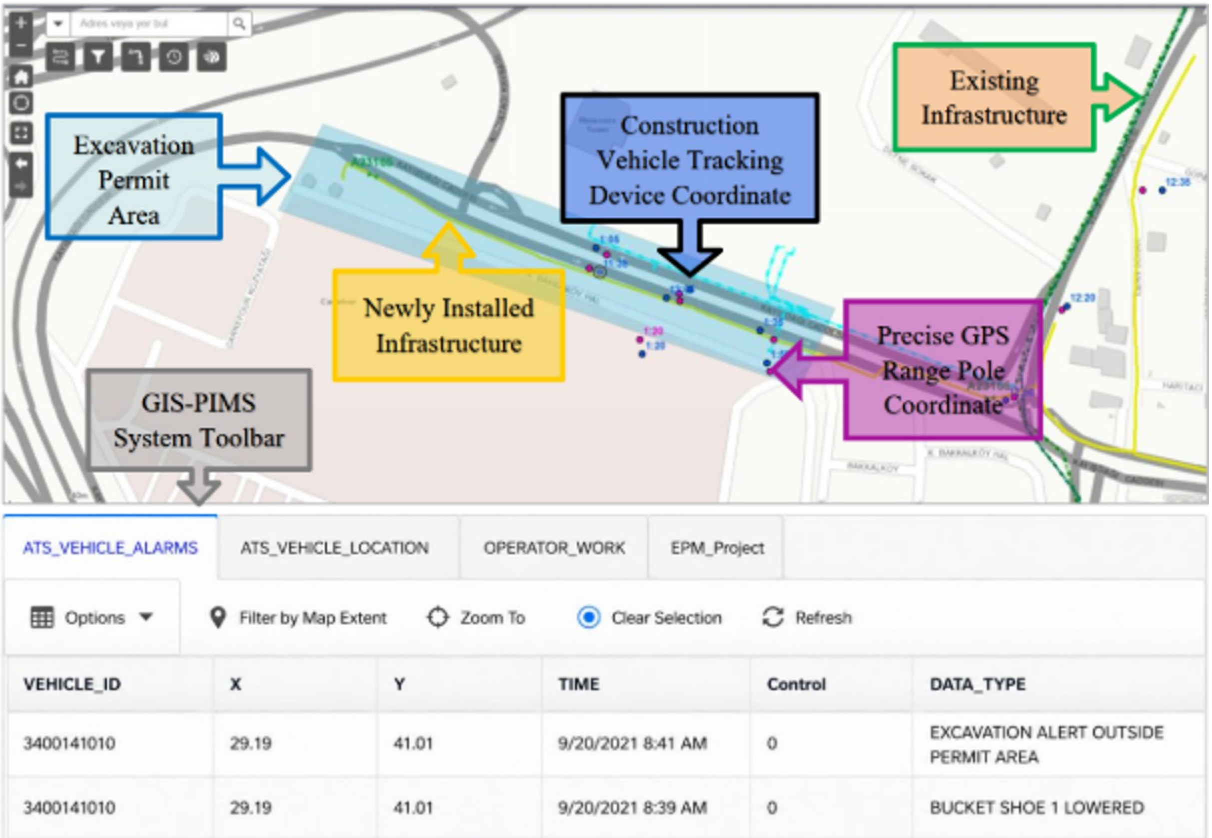

Fig. 8. GIS-PIMS visualization of the buffered excavation permit corridor, underground utility layers, and paired tracking/reference points used for field validation.

		Excavation vehicle tracking device coordinates	RTK-GNSS coordinates	Deviation	Distance to critical utility line			
		(a)	(b)	(a-b)	(Excavator tracking)	(RTK-GNSS)		
#	Time	(latitude, longitude)	(latitude, longitude)	(m)	(m)	(m)	Alarms	Alarm conditions
1	10:10	40.989777 N, 29.195778E	40.98975 N, 29.19576E	3.35	1.04	0.73	Excavation near infrastructure	True Positive (TP)
2	10:25	40.98975 N, 29.195754E	40.98981 N, 29.195818E	8.55	1.14	1.23	Excavation near infrastructure	True Positive (TP)
3	10:40	40.98975 N, 29.195755E	40.98974 N, 29.19577E	1.66	1.12	0.58	Excavation near infrastructure	True Positive (TP)
4	10:55	40.98969 N, 29.19541E	40.989706 N, 29.195392E	2.37	N/A	N/A	Unlicensed excavation warning	True Positive (TP)
5	11:10	40.98963 N, 29.195227E	40.989682 N, 29.19517E	7.49	N/A	N/A	Unlicensed excavation warning	True Positive (TP)
6	11:25	40.989962 N, 29.19592E	40.98992 N, 29.19589E	5.27	0.72	1.21	Excavation near infrastructure	True Positive (TP)
7	11:40	40.989896 N, 29.195791E	40.989861 N, 29.19566E	11.68	7.27	14.5	Compliant operation (no alarm required)	True Negative (TN)
8	11:55	40.989855 N, 29.195965E	40.989764 N, 29.195998E	10.48	N/A	N/A	Unlicensed excavation warning	True Positive (TP)
9	12:10	40.989812 N, 29.195502E	40.989837 N, 29.195545E	4.51	N/A	N/A	Unlicensed excavation warning	True Positive (TP)
10	12:25	40.989703 N, 29.195486E	40.98971 N, 29.195572E	7.27	7.89	14.8	Compliant operation (no alarm required)	True Negative (TN)

Table 3. Paired tracking/reference coordinates, horizontal deviations, utility proximity distances, and alarm outcomes for the Niyaz Street case study.

for correctly identified violations or proximity warnings, and True Negative (TN) for compliant operations requiring no alarm) based on benchmark RTK-GNSS positioning and field validation logs.

Field measurements indicated that the third-party tracking device provided meter-level positioning accuracy under the tested urban operating conditions. For the Niyaz Street dataset ($n = 10$), the horizontal deviation between the tracking-device outputs and the survey-grade GNSS reference measurements ranged from 1.66 m to 11.68 m, with a mean deviation of 6.26 m and a root mean square error (RMSE) of 7.04 m. The 95th percentile error was 11.14 m, indicating that 95% of the observed deviations remained below approximately 11 m. The

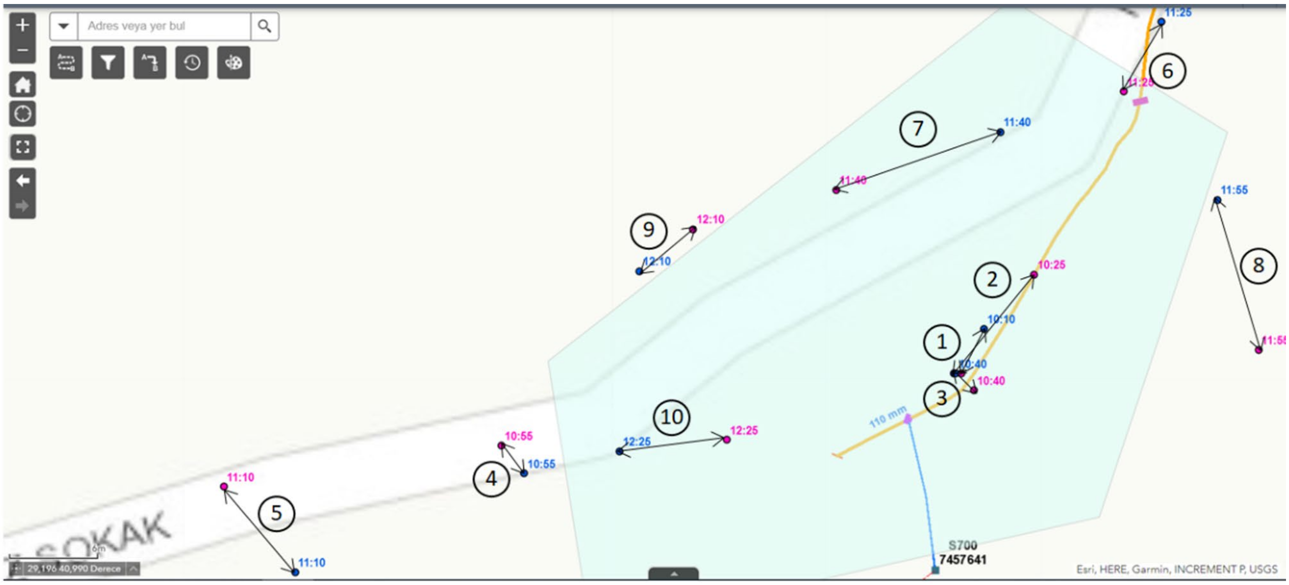

Fig. 9. Spatial distribution of paired tracking and reference points for the Niyaz Street field case study.

#	Time	Excavation vehicle tracking device coordinates	RTK-GNSS coordinates	Deviation	Distance to critical utility line		Alarms	Alarm conditions
		(a)	(b)	(a-b)	(Excavator tracking)	(RTK-GNSS)		
		(latitude, longitude)	(latitude, longitude)	(m)	(m)	(m)		
1	14:40	40.982239 N, 29.091713E	40.982242 N, 29.091731E	1.57	1.37	0.53	Excavation near infrastructure	True Positive (TP)
2	14:55	40.982599 N, 29.089804E	40.98258 N, 29.089864E	5.47	5.83	1.20	Excavation near infrastructure	True Positive (TP)
3	15:10	40.982108 N, 29.08959E	40.98201357 N, 29.08957916E	10.53	2.27	2.61	Excavation near infrastructure	True Positive (TP)
4	15:25	40.982639 N, 29.089686E	40.982656 N, 29.089635E	4.69	N/A	N/A	Unlicensed excavation warning	True Positive (TP)
5	15:40	40.982437 N, 29.091328E	40.982415 N, 29.091302E	3.31	N/A	N/A	Unlicensed excavation warning	True Positive (TP)
6	15:55	40.982187 N, 29.092383E	40.98218667 N, 29.09230291E	6.73	2.78	1.47	Excavation near infrastructure	True Positive (TP)
7	16:10	40.982233 N, 29.092257E	40.98225 N, 29.092177E	6.99	N/A	N/A	Unlicensed excavation warning	True Positive (TP)
8	16:25	40.982226 N, 29.09201E	40.982197 N, 29.092124E	10.14	2.14	0.28	Excavation near infrastructure	True Positive (TP)
9	16:40	40.982133 N, 29.091826E	40.98217 N, 29.091706E	10.84	8.13	11.8	Compliant operation (no alarm required - offline log)	True Negative (TN)
10	16:55	40.982337 N, 29.091226E	40.982328 N, 29.091337E	9.38	2.24	1.05	Excavation near infrastructure	True Positive (TP)

Table 4. Paired tracking/reference coordinates, horizontal deviations, utility proximity distances, and alarm outcomes for the Cebesoy Street case study.

relatively pronounced upper tail of the error distribution suggests that the positioning performance was not uniform across all observations and may intermittently degrade under urban field conditions. This behavior is consistent with known GNSS limitations in built-up environments, where signal occlusion, multipath reflections from surrounding structures, and variations in satellite geometry can increase positioning uncertainty.

Despite these meter-level deviations, the alarm outputs generated during the Niyaz Street test were generally consistent with the spatial conditions represented in the GIS-PIMS platform. Near-utility excavation warnings were generated for points located within close proximity to the critical utility line, whereas unlicensed excavation warnings were generated for points outside the authorized work zone. In addition, no-alarm cases were recorded where the spatial rule set did not require a warning. Therefore, although the maximum positioning deviation reached 11.68 m, the rule-based GIS-PIMS logic was still able to classify the tested excavation related events into the expected operational alarm categories.

Cebesoy Street case study

The results of the Cebesoy Street field test are summarized in Table 4, while Figs. 10 and 11 illustrate the spatial distribution of paired tracking and reference points for the two test segments. Ten paired observations were obtained by simultaneously recording the coordinates reported by the excavation vehicle tracking device and the corresponding reference coordinates measured using the GNSS receiver. The horizontal deviation was calculated

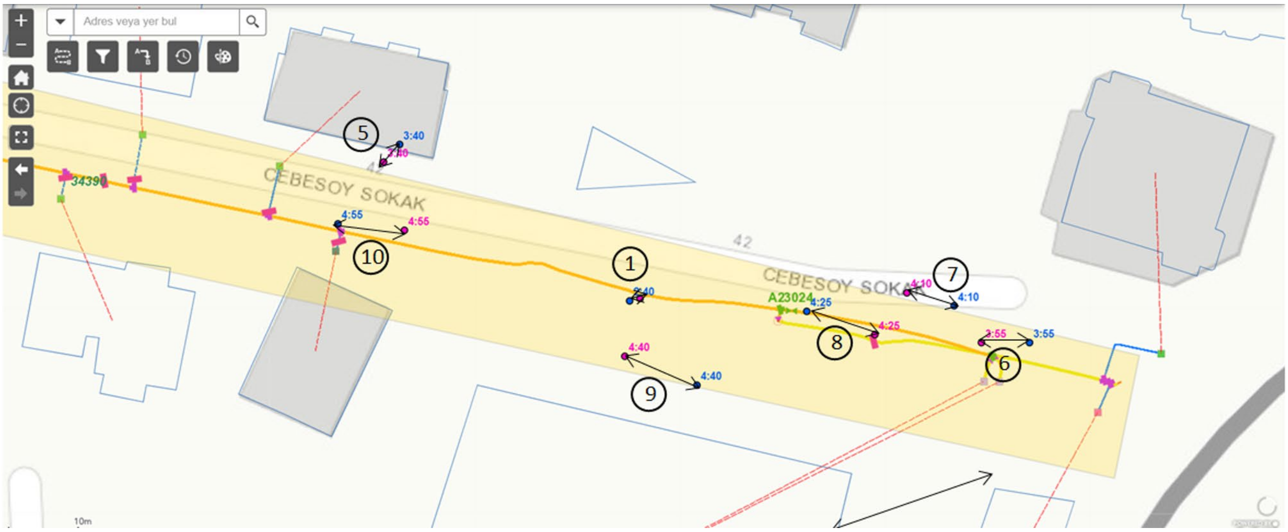

Fig. 10. Spatial distribution of paired tracking and reference points for the Cebesoy Street field case study, Segment 1.

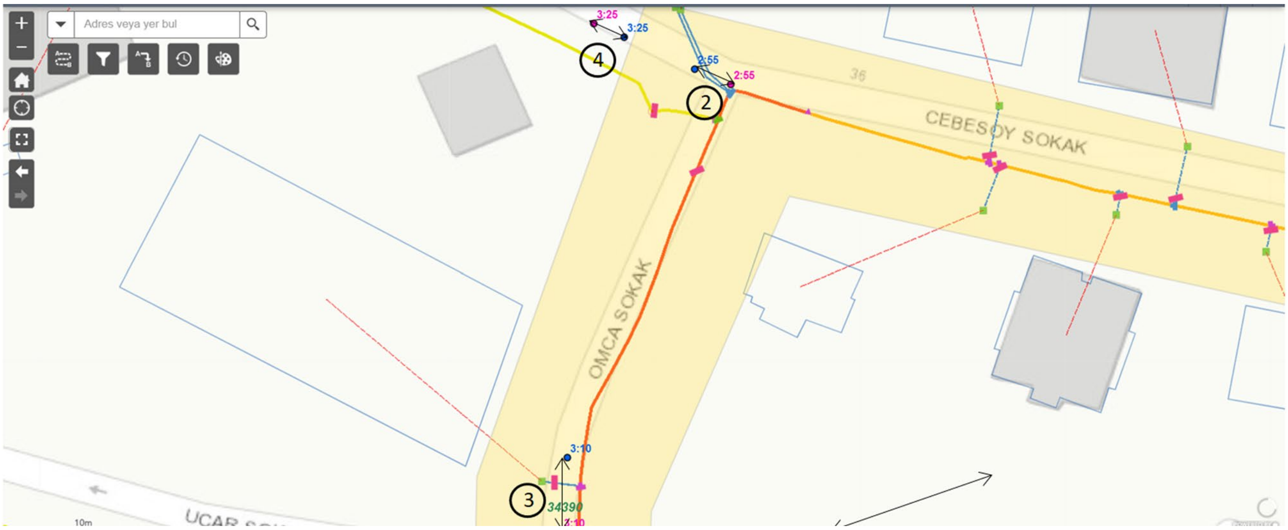

Fig. 11. Spatial distribution of paired tracking and reference points for the Cebesoy Street field case study, Segment 2.

as the planimetric distance between the two coordinate sets. Across the Cebesoy Street dataset, the horizontal deviations ranged from 1.57 m to 10.84 m, with a mean value of 6.97 m, a median of 6.86 m, a root mean square error (RMSE) of 7.61 m, and a 95th percentile value of 10.70 m. To quantitatively evaluate system performance, each observation was classified under "Alarm Conditions" into standard confusion matrix categories (e.g., True Positive (TP) for correctly identified violations or proximity warnings, and True Negative (TN) for compliant operations requiring no alarm) based on benchmark RTK-GNSS positioning and field validation logs.

The occurrence of discontinuous larger deviations indicates that positioning performance may intermittently deteriorate under dense urban conditions, where signal occlusion, multipath reflections from surrounding structures, and reduced satellite visibility can affect GNSS reliability. Despite these meter-level positioning errors, the rule-based GIS-PIMS logic produced the expected operational outcomes for the tested cases. Near-utility excavation alerts were activated when the tracked position indicated proximity to the critical utility line, whereas points outside the authorized work zone were categorized as unlicensed excavation alerts. Notably, one observation did not require an alarm because the operation remained within the permitted work zone and the estimated distance to the critical utility line exceeded the proximity threshold. This record also indicated the absence of cellular connectivity, which is operationally relevant because real-time alarm delivery depends on communication availability.

		Excavation vehicle tracking device coordinates	RTK-GNSS coordinates	Deviation	Distance to critical utility line			
		(a)	(b)	(a-b)	(Excavator tracking)	(RTK-GNSS)		
#	Time	(latitude, longitude)	(latitude, longitude)	(m)	(m)	(m)	Alarms	Alarm conditions
1	11:35	40.98062 N, 29.100699E	40.98064 N, 29.100626E	6.56	2.77	2.95	Excavation near infrastructure	True Positive (TP)
2	11:50	40.98053 N, 29.10134E	40.98051 N, 29.101266E	6.58	27.50	22.7	Compliant operation (no alarm required - offline log)	True Negative (TN)
3	12:05	40.980484 N, 29.101174E	40.980468 N, 29.101267E	8.00	1.90	2.34	Excavation near infrastructure	True Positive (TP)
4	12:20	40.980438 N, 29.104013E	40.98042 N, 29.10398E	3.42	N/A	N/A	Unlicensed excavation warning	True Positive (TP)
5	12:35	40.981058 N, 29.10469E	40.981058 N, 29.104554E	11.4	N/A	N/A	Unlicensed excavation warning	True Positive (TP)
6	12:50	40.979937 N, 29.103581E	40.979954 N, 29.10364E	5.32	2.60	1.82	Excavation near infrastructure	True Positive (TP)
7	13:05	40.980751 N, 29.100674E	40.980715 N, 29.10075E	7.50	15.70	12.40	Compliant operation (no alarm required - offline log)	True Negative (TN)
8	13:20	40.980185 N, 29.100999E	40.980261 N, 29.100982E	8.58	35.60	27.40	Unlicensed excavation warning	True Positive (TP)
9	13:35	40.98031 N, 29.10184E	40.980262 N, 29.101935E	9.57	2.01	0.41	Excavation near infrastructure	True Positive (TP)
10	13:50	40.980137 N, 29.101886E	40.980091 N, 29.101907E	5.42	14.80	18.60	Compliant operation (no alarm required - offline log)	True Negative (TN)

Table 5. Paired tracking/reference coordinates, horizontal deviations, utility proximity distances, and alarm outcomes for the Kayışdağı Avenue case study.

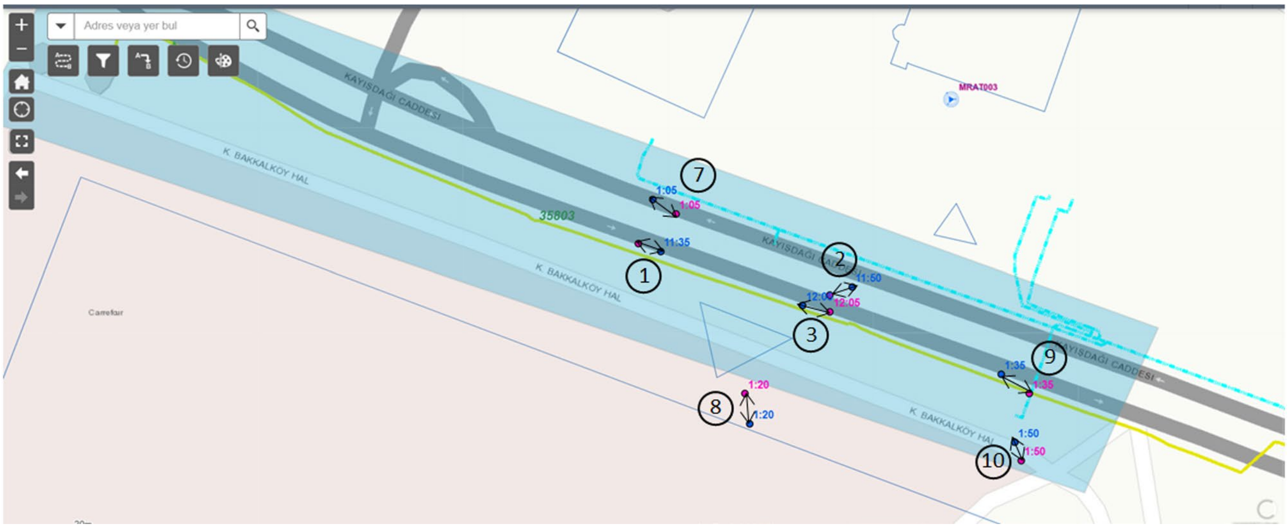

Fig. 12. Spatial distribution of paired tracking and reference points for the Kayışdağı Avenue field case study, Segment 1.

Kayışdağı Avenue case study

The results of the Kayışdağı Avenue field test are presented in Table 5, and the spatial distribution of the paired measurement points across the two test segments is illustrated in Figs. 12 and 13. As in the previous case studies, ten paired observations were obtained by simultaneously recording the coordinates reported by the excavation vehicle tracking device and the corresponding reference coordinates measured using the GNSS receiver. For each observation, the horizontal deviation was calculated as the planimetric distance between the tracking device coordinate and the GNSS reference coordinate. This procedure enabled the positioning performance of the tracking device to be evaluated under another representative urban excavation condition. To quantitatively evaluate system performance, each observation was classified under "Alarm Conditions" into standard confusion matrix categories (e.g., True Positive (TP) for correctly identified violations or proximity warnings, and True Negative (TN) for compliant operations requiring no alarm) based on benchmark RTK-GNSS positioning and field validation logs.

Across the Kayışdağı Avenue dataset, the horizontal deviations ranged from 3.42 m to 11.40 m, with a mean value of 7.24 m, a median of approximately 7.04 m, an RMSE of 7.56 m, and a 95th percentile value of approximately 10.58 m.

The Kayışdağı Avenue case study also showed meter-level positioning deviations under urban field conditions. The alarm outputs included near-utility excavation warnings, unlicensed excavation warnings, and no-alarm cases where the operation remained within the permitted area or outside the proximity threshold. Similar to the

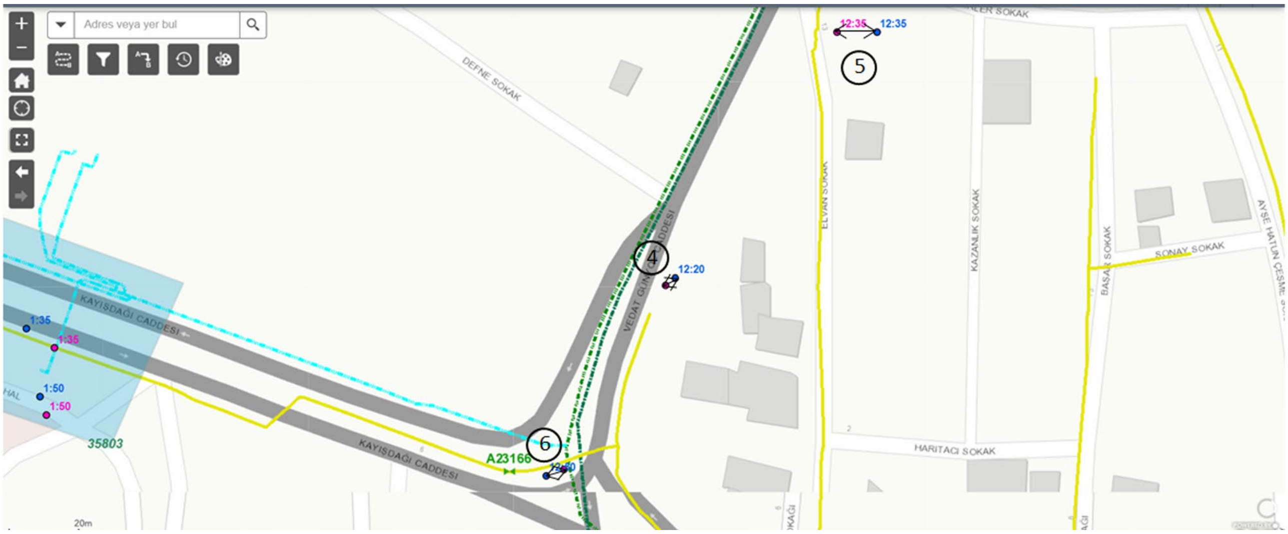

Fig. 13. Spatial distribution of paired tracking and reference points for the Kayışdağı Avenue field case study, Segment 2.

Actual condition \ predicted status	Alarm/violation detected (positive)	No alarm required/normal (negative)	Total
Actual alarm condition (violation/proximity)	24 (TP)	0 (FN)	24
Actual normal condition (no violation)	1 (FP)	5 (TN)	6
Total	25	5	30

Table 6. Confusion matrix for the GIS-PIMS excavation activity and rule-based alarm system ($n = 30$).

Performance metric	Mathematical formula	Calculated value (%)	Operational Interpretation
Overall Accuracy	(TP + TN) / Total	96.7	High overall effectiveness in identifying alarm vs. non-alarm conditions.
Precision (PPV)	TP / (TP + FP)	96	High proportion of generated alarms corresponding to true field violations.
Sensitivity (Recall)	TP / (TP + FN)	100	Perfect capability in capturing all active excavation threats and violations.
Specificity (TNR)	TN / (TN + FP)	83.3	Ability to correctly identify compliant, non-risky excavation operations.
False Positive Rate (FPR)	FP / (TN + FP)	16.7	Rate of false alarms caused primarily by meter-level GNSS positioning uncertainty.
False Negative Rate (FNR)	FN / (TP + FN)	0	Zero missed alarms across the evaluated field observations.

Table 7. Quantitative performance indicators of the alarm and detection system.

other two sites, these results indicate that the rule-based GIS-PIMS logic can classify excavation-related spatial events under different urban corridor conditions. However, the presence of deviations exceeding the 6 m device threshold confirms that proximity-based warnings should be interpreted with verification support.

System detection and alarm performance evaluation

To quantitatively evaluate the operational reliability of the proposed GIS-PIMS framework, the rule-based alarm and activity detection outputs were benchmarked against survey-grade RTK-GNSS reference coordinates and verified field logs across the 30 paired observations. Active excavation states were classified using a combined sensor logic integrating stabilizer-leg position, boom motion, and operator seat occupancy. An operational alarm condition was designated as a true positive (TP) when active excavation occurred near critical infrastructure (< 6 m) or outside the authorized permit corridor and was correctly flagged by the system.

Across the 30 evaluated instances, the system achieved an overall classification accuracy of 96.7%. A total of 24 true positives (TP), 5 true negatives (TN), 1 false positive (FP), and 0 false negatives (FN) were observed. The single false positive instance occurred at a location close to the permit corridor boundary, where the tracking device's positioning deviation (RMSE = 7.41 m) caused the system to trigger an out-of-permit boundary alert. While intermittent cellular offline states (NO SIM) occurred during field testing, these events coincided with compliant in-license operations and thus did not result in missed alarm conditions (FN = 0). Standard performance metrics were calculated as follows: Precision = 96.0%, Sensitivity (Recall) = 100.0%, Specificity = 83.3%, False Positive Rate (FPR) = 16.7%, and False Negative Rate (FNR) = 0.0%. The updated confusion matrix and detailed performance indicators are summarized in Tables 6 and 7.

Buffer corridor width (m)	False positive risk (false alarms)	Missed violation risk (false negatives)	Operational evaluation & applicability
5–10	High (40–50%)	Very Low (0–2%)	Unsuitable for standard fleet tracking due to GNSS noise (RMSE 7.41 m) causing persistent false alerts
15	Moderate (15–20%)	Low (3%)	Acceptable for wider arterials; requires camera-assisted validation near boundary limits
20	Low (3.3% – 1/30)	Low (0.0% – 0/30)	Optimal threshold for urban corridors; accommodates 95th percentile GNSS error (11.15 m)
25–30	Very Low (0%)	High (15–25%)	Overly permissive; fails to detect unauthorized excavations near strict right-of-way boundaries

Table 8. Sensitivity analysis of geofence corridor buffer sizes relative to positioning uncertainty.

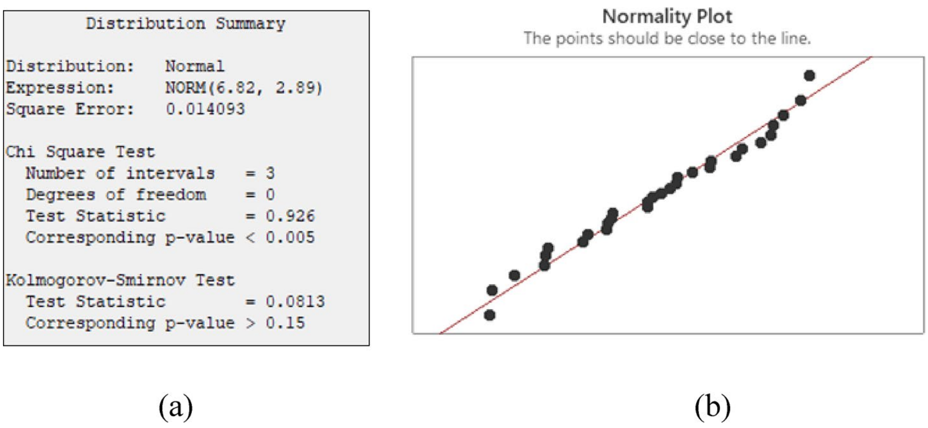

Fig. 14. Normality assessment of horizontal positioning deviations (**a**) one-sample Kolmogorov–Smirnov test results (D = 0.0813, $p > 0.15$) and (**b**) normal probability plot.

Sensitivity analysis of geofencing buffer widths and positioning uncertainty

To address the operational impact of the observed positioning errors (mean = 6.82 m, RMSE = 7.41 m, 95th percentile = 11.15 m), a sensitivity analysis was conducted across varying geofenced buffer widths (5 m to 30 m) along the utility corridor. Given that urban street corridors often exhibit widths between 10 m and 20 m, spatial threshold selection directly affects the trade-off between false alarm generation and missed boundary violations.

As detailed in Table 8, buffer corridors between 5 m and 10 m suffer from elevated false positive rates (FPR = 40–50%) due to standard urban GNSS multipath deviations exceeding the narrow corridor boundaries. Conversely, expanding the buffer corridor to 25–30 m eliminates false alarms but introduces a high risk of missed detections (15–25%), where unauthorized excavations near corridor edges remain unflagged. The 20 m buffer corridor selected in this study represents the optimal trade-off for urban streetworks, maintaining low false alarm rates while successfully capturing boundary compliance.

Overall positioning performance and statistical assessment

After completing the site specific evaluations, the positioning results from the three field case studies were combined and analyzed as a single validation dataset. In total, thirty paired observations were collected from Niyaz Street, Cebesoy Street, and Kayışdağı Avenue, as summarized in Tables 3, 4 and 5. Differences were observed between the coordinates reported by the third party tracking device and those measured using the GNSS receiver. For the combined dataset, the overall mean horizontal deviation was 6.82 m, with a standard deviation of 2.94 m and a range of 1.57–11.68 m. These values indicate that the tracking device exhibited meter level positioning performance under urban operating conditions.

The observed deviations are likely associated with both the actual positioning capability of the device and environment related GNSS error sources, including signal occlusion, multipath reflections in built-up street corridors, variations in satellite geometry, and atmospheric effects. Accordingly, this level of positioning uncertainty supports the use of buffered permit corridors and camera-assisted verification within the GIS-PIMS workflow. From an operational perspective, such uncertainty is particularly relevant for geofencing-based permit control and near utility warning logic, where spatial decisions depend directly on the accuracy and stability of the tracking output.

The combined dataset was subjected to normality assessment to further evaluate the distributional behavior of the horizontal deviation data. A one-sample Kolmogorov–Smirnov test indicated no statistically significant deviation from normality (D = 0.0813, $p > 0.15$). This finding was also supported by the normal probability plot, in which the observed deviations were generally aligned with the reference line. Therefore, the normal approximation was considered suitable for descriptive interpretation of the positioning-error distribution (Fig. 14).

The distribution of horizontal deviations was then evaluated relative to the tracking device's specified 6 m deviation limit. The observed exceedance rate was 60%, with 18 of the 30 measurements exceeding the 6 m threshold (USL = 6.0 m). For comparative interpretation, the expected exceedance rate under the fitted normal model was estimated using the sample mean of 6.823 m and the standard deviation of 2.936 m, resulting in an expected exceedance rate of 61.0%. The close agreement between the observed and model based exceedance rates indicates that deviations greater than 6 m were not isolated outliers, but rather a frequent characteristic of the tracking device under the tested urban field conditions (Fig. 15).

These findings indicate that the tracking device can support general permit-corridor monitoring when appropriate buffer distances are used. However, the frequent exceedance of the 6 m deviation limit shows that proximity-based warning thresholds require additional verification, as discussed in the following section.

Operational implications for geofencing, utility protection, and pavement reinstatement

The observed meter level positioning errors have important implications for the practical use of GIS-PIMS in excavation monitoring and municipal decision-making. Across the combined validation dataset, the tracking device produced a mean horizontal deviation of 6.82 m, an RMSE of 7.41 m, and a 95th percentile error of 11.15 m. These values indicate that the system can support corridor level excavation monitoring, provided that permit and proximity-based alarms are interpreted with consideration of positioning uncertainty under dense urban conditions.

Benchmarking against existing positioning technologies indicates that the tested device performs within the general meter-level range expected from standard GNSS-based fleet tracking solutions. In comparison, DGNSS/DGPS systems can provide improved meter- or sub-meter-level positioning, whereas RTK/NRTK GNSS systems can achieve centimeter-level accuracy under suitable operating conditions. However, these higher-precision technologies generally require correction services, compatible hardware, reliable communication links, greater implementation complexity and higher implementation costs. Therefore, the tested tracking device should not be interpreted as a substitute for survey-grade or RTK GNSS. Its principal advantage lies in providing a low-cost, continuously connected positioning input integrated with excavation activity sensors, permit geometries, utility layers, and automated GIS-based alerts. Based on the observed positioning performance, the tested configuration is more appropriate for corridor-scale monitoring and precautionary warning than for enforcement-level decisions close to narrow permit boundaries. A comparative summary of these technologies is presented in Table 9.

As summarized in Table 9, the tested GIS-PIMS configuration is suitable for corridor-scale excavation monitoring and for generating precautionary alerts when excavation activity approaches critical underground utilities. These alarms are intended to trigger operator attention and supervisory verification rather than provide definitive utility clearance. DGNSS/DGPS or RTK/NRTK technologies may be integrated where narrower geofence tolerances, higher-precision spatial confirmation, or enforcement-level positioning is required.

From a permit compliance perspective, the achieved accuracy is generally compatible with the proposed geofencing strategy. In the pilot implementation, the authorized excavation area was represented by a buffered corridor of approximately 20 m around the planned infrastructure alignment. Since the observed 95th percentile error remained below this corridor width, the system can support inside/outside permit verification for most

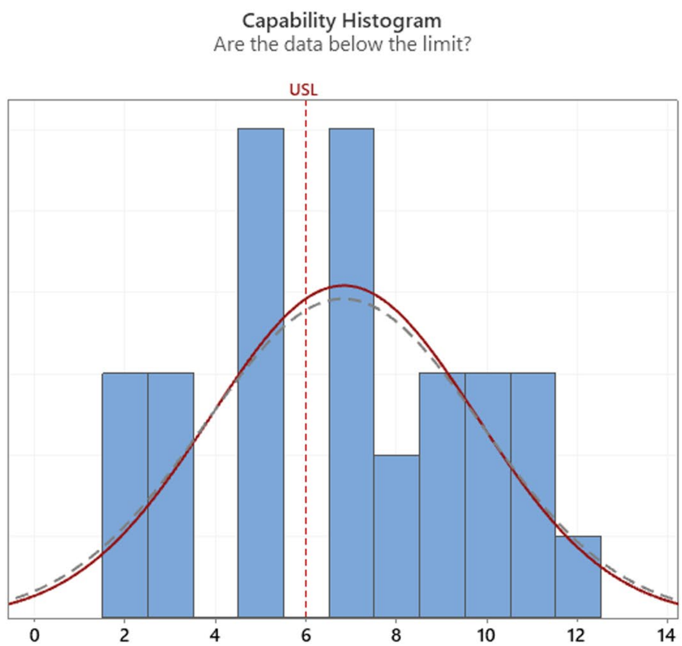

Process Characterization	
Total N	30
Subgroup size	1
Mean	6,823
Standard deviation (overall)	2,9363
Standard deviation (within)	3,0569

Capability Statistics	
Actual (overall)	
Pp	*
Ppk	-0,09
Z.Bench	-0,28
% Out of spec (observed)	60,00
% Out of spec (expected)	61,04
PPM (DPMO) (observed)	600000
PPM (DPMO) (expected)	610372
Potential (within)	
Cp	*
Cpk	-0,09
Z.Bench	-0,27
% Out of spec (expected)	60,61
PPM (DPMO) (expected)	606124

Fig. 15. Observed and normally fitted distribution of horizontal positioning deviations relative to the 6 m device accuracy threshold.

Technology	Typical horizontal accuracy	Main urban limitations	Suitability for GIS–PIMS applications
Standard GNSS Fleet tracker	Approximately 2.50–10.00 + meter	Multipath Signal occlusion Limited satellite visibility Antenna-installation effects	Corridor-scale monitoring Equipment tracking
DGNSS/DGPS	Sub-meter to several meters	Dependence on correction-data availability and communication coverage	Improved geofence discrimination Permit-boundary monitoring
RTK/NRTK GNSS	Centimeter-level under suitable conditions	Correction-link interruption Loss of fixed solution Multipath Open-sky requirements	High-precision boundary control Near-utility position confirmation
Proposed GIS–PIMS configuration	Mean deviation: 6.82 m; RMSE: 7.41 m;	Urban GNSS uncertainty Possible communication interruptions	Corridor-scale permit monitoring and precautionary near-utility warning with camera or supervisory verification

Table 9. Benchmark comparison of positioning technologies for GIS–PIMS applications. Note: The benchmark accuracy ranges are indicative and may vary depending on receiver quality, antenna configuration, correction-service availability, satellite visibility, urban morphology, and the statistical accuracy metric used.

operational cases. However, excavations close to permit boundaries may occasionally produce false or vague alarms. Therefore, camera assisted verification and visual inspection may be needed to confirm alarm conditions before enforcement decisions are made.

Proximity-based warnings near critical underground utilities require a more conservative interpretation. The 6 m threshold used for near utility alerts is close to the observed mean positioning deviation and may be exceeded under adverse GNSS conditions. Thus, these alarms should be regarded as early warning indicators rather than definitive clearance assessments. Their main purpose is to prompt operator attention and supervisory review when excavation activity is detected near critical infrastructure such as natural gas, water, fiber-optic, or energy lines. The integration of GNSS quality filtering, temporal decision logic, visual feeds, and field inspection can further improve the reliability of such safety-critical alarms.

Communication reliability represents an additional operational consideration for GIS-PIMS. Several field records indicated the absence of cellular connectivity, showing that real-time transmission of alarms and event data may not be continuously available under all operating conditions. A communication interruption may delay the delivery of warnings to responsible authorities and limit immediate supervisory intervention. Therefore, practical deployments should incorporate communication-status monitoring, local data buffering, delayed synchronization after network recovery, and a dedicated communication-failure notification.

Beyond alarm generation, GIS-PIMS can support proactive pavement reinstatement management. The identification of excavation commencement and location could help authorities schedule inspections and reinstatement actions more efficiently. Time-stamped excavation logs and geofenced event records could be used as inputs for maintenance triggers, including inspection requests, temporary patching records, and permanent reinstatement planning. These records can also support monitoring of the elapsed time between excavation completion, temporary patching, and permanent asphalt reinstatement, thereby helping authorities identify prolonged exposure to open trenches or temporary surfaces. By identifying the responsible operator, excavation date, and exact work location, GIS-PIMS could enable municipalities to relate excavation activities to subsequent pavement defects, accident records, user complaints, and maintenance interventions.

It should be noted that the pilot deployment recorded excavation-related locations, timestamps, permit conditions, and alarm outcomes but did not directly measure pavement-condition indicators such as the Pavement Condition Index (PCI), International Roughness Index (IRI), rutting, or patch-edge cracking. GIS-PIMS should therefore be regarded as an operational decision-support framework for supporting reinstatement workflows rather than as a direct pavement-distress measurement system. This distinction is important because delayed or inadequate reinstatement may contribute to localized settlement, patch-edge cracking, surface roughness, abrupt surface discontinuities, and longer-term pavement defects. Such conditions may reduce ride quality, increase speed variability, and induce sudden braking, lane-changing, or evasive maneuvers, particularly among vulnerable road users such as motorcyclists and cyclists. Accordingly, linking excavation records with inspection and reinstatement workflows may provide a data-driven basis for municipal pavement management and subsequent assessment of pavement serviceability and traffic-safety outcomes.

At the network level, centralized excavation monitoring can improve coordination among utility agencies and municipal authorities. A shared GIS-PIMS platform provides real-time visibility of excavation locations, routes, activity status, permit conditions, proximity warnings, and alarm records. This shared situational awareness can reduce repeated or conflicting interventions in the same corridor, prevent multiple sequential cuts on newly restored pavements, minimize unnecessary lane occupancy, and support better work-zone planning. The time-stamped geospatial inspection trail may also improve accountability by documenting excavation activity details (where, when, and by whom) were performed, thereby supporting post-event investigation, cost recovery, standardized documentation, and collaboration among related agencies.

Overall, GIS-PIMS should be interpreted not only as a vehicle tracking system but also as a spatial decision-support system for excavation governance, utility protection, and pavement management. While the current positioning performance is sufficient for corridor-scale monitoring, safety-critical proximity warnings require conservative interpretation and additional verification. With higher accuracy positioning hardware, GNSS quality control, temporal alarm logic, and camera assisted confirmation, the framework can contribute to reduced unauthorized excavations, fewer service disruptions, more timely pavement reinstatement, safer traffic operations, improved user satisfaction, and enhanced urban infrastructure resilience.

The capabilities directly evaluated in the present pilot study include the positioning performance of the tracking device, the recording of utility-proximity distances, rule-based alarm accuracy ($n = 30$), and the integration of permit and utility layers within the GIS-PIMS environment. However, while the initial alarm performance was quantified using the pilot dataset, comprehensive statistical evaluation of activity detection across varied equipment types, long-term cellular communication performance, and camera-assisted visual confirmation warrants further investigation through larger-scale field studies.

Conclusions

This study developed and pilot field-tested a Geographic Information System–based Pavement and Infrastructure Monitoring System (GIS-PIMS) to enhance permit compliance and support municipal pavement management during urban utility excavations. The proposed framework combines sensor-based excavation activity detection, GNSS-based equipment positioning, GIS-based permit geometries, underground utility layers, and rule-based alarm logic. In this way, GIS-PIMS links excavation monitoring with permit compliance, utility protection, and pavement asset management.

The field case studies demonstrated that the system could record excavation-related spatial events, generated rule-based near-utility and out-of-permit alarm outcomes, and produced auditable geospatial records under the tested urban conditions. Across 30 paired observations collected at three sites, the tracking device produced meter-level positioning deviations, with a mean horizontal deviation of 6.82 m, an RMSE of 7.41 m, and a 95th percentile error of 11.15 m. The observed exceedance rate above the 6 m device limit was 60%, close to the 61.0% estimated under the fitted normal model.

The 20 m-wide permit corridor used in the pilot, defined by a 10 m lateral offset on each side of the planned utility centerline, provided an operational basis for general inside/outside permit classification under the tested conditions. However, its suitability should not be interpreted as universally optimal because geofence performance depends on corridor geometry, positioning uncertainty, street morphology, and the distance of individual observations from the permit boundary. Near-utility warnings based on the 6 m proximity threshold should therefore be regarded as precautionary alerts rather than definitive clearance assessments. GNSS-quality filtering, temporal confirmation, camera-assisted verification, and field inspection are needed for safety-critical decisions.

From a pavement-management perspective, the principal contribution of GIS-PIMS is the creation of a geospatial and temporal audit trail that may support inspection scheduling, temporary-patching records, permanent reinstatement planning, post-event investigation, responsibility assignment, and cost recovery. These records may also enable authorities to associate excavation activities with subsequent pavement defects, complaints, accidents, and maintenance interventions. By linking excavation records with reinstatement workflows, the framework may help authorities identify prolonged exposure to open trenches or temporary surfaces and support more timely pavement-restoration actions.

Nevertheless, the study did not directly measure pavement-condition or serviceability indicators, including the Pavement Condition Index, International Roughness Index, rutting, settlement, or patch-edge cracking. Potential improvements in reinstatement timeliness, pavement performance, traffic safety, and infrastructure resilience should be interpreted as downstream applications requiring longitudinal evaluation.

At the network level, GIS-PIMS may support improved coordination among utility agencies and related authorities. A shared platform can reduce repeated or conflicting excavations in the same corridor, prevent sequential cuts on newly restored pavements, and support more rational scheduling of pavement reinstatement and maintenance interventions. Thus, the system should be regarded not only as a vehicle tracking tool, but also as a data driven framework intended to support pavement-asset protection and urban road maintenance planning.

The principal limitation of the pilot implementation is the positioning uncertainty of the tracking device under dense urban GNSS conditions. Signal occlusion, multipath reflections, reduced satellite visibility, and variations in satellite geometry may reduce spatial reliability, especially for narrow proximity thresholds. In addition, the validation dataset was limited to 30 paired observations from three urban field sites. Broader validation is needed across different pavement types, road classes, excavation geometries, traffic conditions, and urban morphologies.

Future work should focus on improving positioning reliability and strengthening the integration with pavement management systems. Higher accuracy GNSS hardware, GNSS quality indicators, temporal alarm filtering, and front/rear camera verification should be incorporated to reduce false alarms. Additionally, while the present study established the geospatial tracking and compliance workflow, future research will concentrate on direct field measurements of pavement serviceability and distress indicators (such as Pavement Condition Index (PCI) and International Roughness Index (IRI)) over longitudinal monitoring periods. Larger citywide deployments involving multiple utility agencies and construction machineries would allow GIS-PIMS to be evaluated as a scalable smart pavement management tool for reducing unauthorized excavations, improving reinstatement compliance, preserving pavement performance, and enhancing urban infrastructure resilience. Urban implementations should also be supported by operator training, standardized pavement reinstatement quality-control procedures, and a compliance regime capable of identifying recurrent non-compliance.

Data availability

All data supporting the findings of this study are available within the paper.

Received: 27 May 2026; Accepted: 7 September 2026

References

1. Zou, C., Zhu, R., Tao, Z., Ouyang, D. & Chen, Y. Evaluation of building construction-induced noise and vibration impact on residents. *Sustainability* **12**, 1579 (2020). https://doi.org/10.3390/su12041579
2. Rönkä, K., Ritola, J. & Rauhala, K. Underground space in land-use planning. *Tunn. Undergr. Sp Technol.* **13**, 39–49 (1998). https://doi.org/10.1016/S0886-7798(98)00029-7
3. Curiel-Esparza, J., Canto-Perello, J. & Calvo, M. A. Establishing sustainable strategies in urban underground engineering. *Sci. Eng. Ethics* **10**, 523–530 (2004). https://doi.org/10.1007/s11948-004-0009-5
4. Goodman, A. S. & Hastak, M. *Infrastructure Planning Handbook: Planning, Engineering, and Economics* (2006).
5. Liu, W. et al. Alleviating corporate environmental pollution threats toward public health and safety: The role of smart city and artificial intelligence. **143** (2021).
6. Arudi, R., Pickering, B. & Flading, J. Planning and implementation of a management system for utility cuts. *Transp. Res. Rec J. Transp. Res. Board* **1699**, 42–48 (2000). https://doi.org/10.3141/1699-06
7. Eskandari Torbaghan, M. et al. Investigating the relationship between trenching practice and road deterioration. *Infrastruct. Asset Manag.* **7**, 282–296 (2020). https://doi.org/10.1680/jinam.19.00052
8. Transport Infrastructure Ireland (TII). *Pavement Assessment, Repair and Renewal Principles (AM-PAV-06050)*. http://www.tiipublications.ie (2020).
9. Mallela, J. & Sadasivam, S. *Work Zone Road User Costs: Concepts and Applications* (2011).
10. Schroeder, B. J. et al. *Delay and User Cost Estimation for Work Zones on Urban Arterials (NCDOT Project 2013-09 Final Report)* (2015).
11. Wang, T., Harvey, J., Lea, J. & Kim, C. Impact of pavement roughness on vehicle free-flow speed. *J. Transp. Eng.* **140**, 1–11 (2014). https://doi.org/10.1061/(ASCE)TE.1943-5436.0000689
12. Wilde, W. J., Grant, C. A. & Nelson, P. K. *Manual for Controlling and Reducing the Frequency of Pavement Utility Cuts. Report No. FHWA-IF-02-064* (Federal Highway Administration, U.S. Department of Transportation, 2018).
13. Ghosh, D., Dunn, S. M. & Petersen, L. Utility cut impact assessment and fee development using pavement management system. *Transp. Res. Rec.* **2679**, 33–43 (2025). https://doi.org/10.1177/03611981241287194
14. Coni, M., Portas, S., Rombi, J., Mereu, P. & Maltinti, F. Evaluation of utility cut patching on pavement structure. In *Computational Science and Its Applications—ICCSA 2024 Workshops* (eds Gervasi, O. et al.) 48–61. https://doi.org/10.1007/978-3-031-65332-2_4 (Springer, 2024).
15. Clarke, R. J. Planning and mapping of underground space—an overview. *Tunn. Undergr. Sp Technol.* **15**, 271–286 (2000). https://doi.org/10.1016/S0886-7798(00)00056-0
16. Yumrutas, H. I. & Iyinam, S. A GIS based decision support system proposal for planning infrastructure excavations: Fatih district example. *Sak Univ. J. Sci.* **22**, 401–416 (2018). https://doi.org/10.16984/saufenbilder.292668
17. Apak, M. Y., Ozen, H., Calis, M., Golgeli, B. & Ataoglu, S. Applications of utility tunnels for natural gas pipelines. *Tunn. Undergr. Sp Technol.* **122**, 104243 (2022). https://doi.org/10.1016/j.tust.2021.104243
18. Venigalla, M. M. & Baik, B. H. GIS-based engineering management service functions: taking GIS beyond mapping for municipal governments. *J. Comput. Civ. Eng.* **21**, 331–342 (2007).
19. Balasubramani, B. S., Badhrudeen, M., Derrible, S. & Cruz, I. Smart data management of urban infrastructure using geographic information systems. *J. Infrastruct. Syst.* **26**, 06020002 (2020). https://doi.org/10.1061/(ASCE)IS.1943-555X.0000582
20. Tseng, S. M., Chou, C. C., Ho, T. W., Lin, C. Y. & Chen T.-C. A spatiotemporal database approach to the management of utility work schedules in transportation projects. *Autom. Constr.* **20**, 729–739 (2011). https://doi.org/10.1016/j.autcon.2011.01.004
21. Quiroga, C. & Pina, R. Issues in automating utility permits at transportation agencies. *Transp. Res. Rec* 143–151. https://doi.org/10.3141/1890-17;CTYPE:STRING:JOURNAL (2004).
22. Xu, X., Chen, K. & Cai, H. Automating utility permitting within highway right-of-way via a generic UML/OCL model and natural language processing. *J. Constr. Eng. Manag.* **146**, 04020135 (2020). https://doi.org/10.1061/(ASCE)CO.1943-7862.0001936
23. Angelidou, M. Four European Smart City Strategies. *Int. J. Soc. Sci. Stud.* **4**, 18–30 (2016). https://doi.org/10.11114/ijsss.v4i4.1364
24. Axelsson, K. & Granath, M. Stakeholders' stake and relation to smartness in smart city development: Insights from a Swedish city planning project. *Gov. Inf. Q.* **35**, 693–702 (2018). https://doi.org/10.1016/j.giq.2018.09.001
25. Simonofski, A., Vallé, T., Serral, E. & Wautelet, Y. Investigating context factors in citizen participation strategies: A comparative analysis of Swedish and Belgian smart cities. *Int. J. Inf. Manage.* **56**, 102011 (2021). https://doi.org/10.1016/j.ijinfomgt.2019.09.007
26. Rao, A. S. et al. Real-time monitoring of construction sites: Sensors, methods, and applications. *Autom. Constr.* **136**, 104099 (2022). https://doi.org/10.1016/j.autcon.2021.104099
27. Einizinab, S. et al. Enabling technologies for remote and virtual inspection of building work. *Autom. Constr.* **156**, 105096 (2023). https://doi.org/10.1016/j.autcon.2023.105096
28. Talmaki, S. & Kamat, V. R. Real-time hybrid virtuality for prevention of excavation related utility strikes. *J. Comput. Civ. Eng.* **28**, 1–17 (2014). https://doi.org/10.1061/(asce)cp.1943-5487.0000269
29. Asadollahi, S., Scholtenhuis, L., olde, Vahdatikhaki, F. & Dorée, A. Geofencing-based safety system for high-pressure pipelines (2018).

Acknowledgements

The author extends gratitude to IGDAS and Project Update Unit for their valuable contributions. Appreciation is also expressed to the project team for their support during field deployment and assistance with data collection. Furthermore, the author acknowledges the use of generative artificial intelligence (GenAI) tools for assistance with language editing and figure preparation.

Author contributions

Conceptualization, methodology, validation, formal analysis, investigation, resources, data curation, visualization, project administration, and writing—original draft preparation were performed by M.Y.A. The author reviewed and approved the final manuscript.

Funding

This study was funded by IGDAS Research and Development Center, under R&D Project No.8: I-MATS Construction Machinery Tracking System (GIS-Based Excavator Tracking and Excavation Violation Detection System).

Declarations

Competing interests
The authors declare no competing interests.

Additional information
Correspondence and requests for materials should be addressed to M.Y.A.